9 Palau

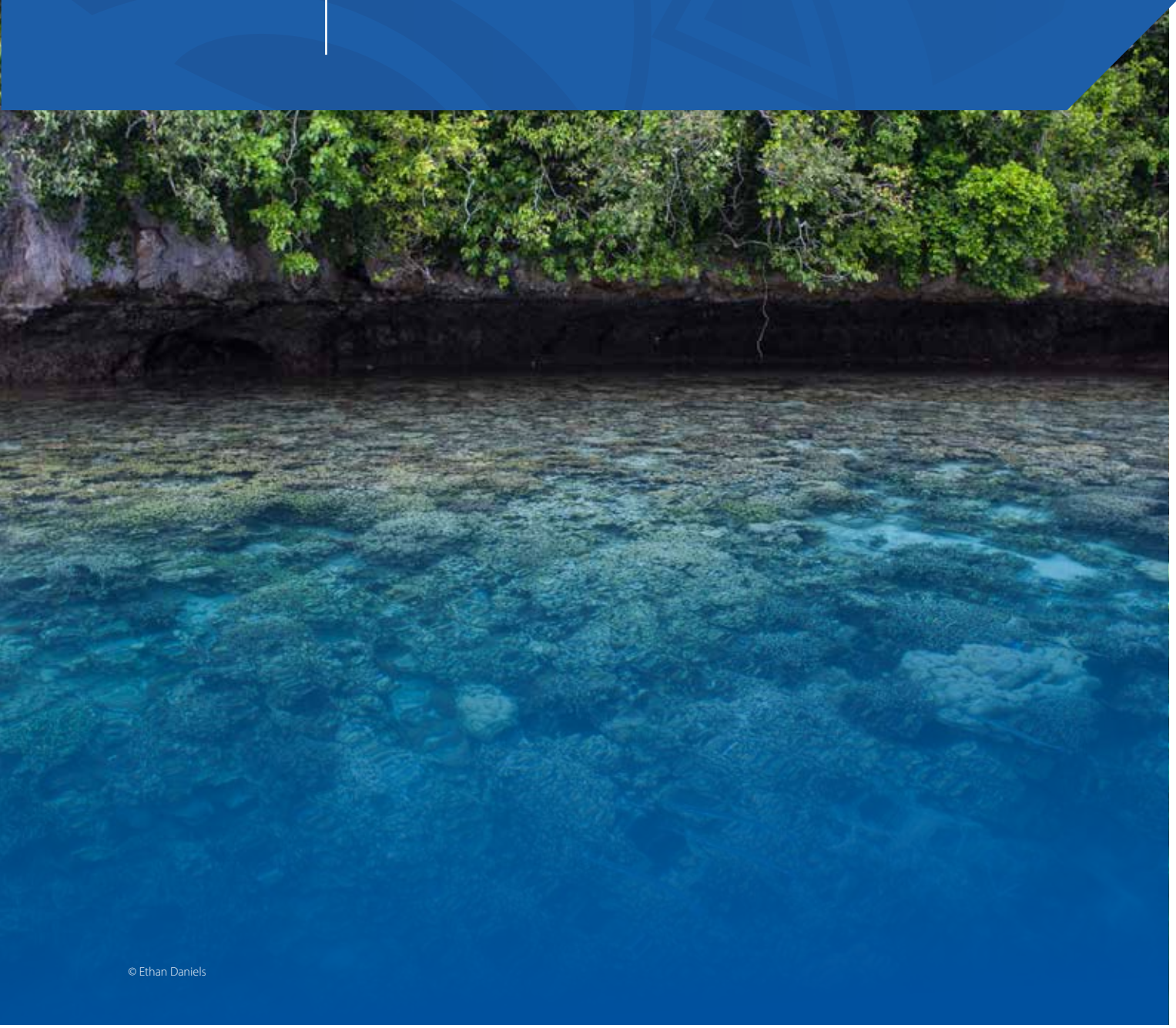

© Ethan Daniels

9.1 Summary

9.1.1 Climate

- There is little seasonal variation in air temperature, which is strongly linked to changes in the surrounding ocean temperature. Palau's wet season is from May to October.
- There is a year-round impact on rainfall from the Intertropical Convergence Zone (ITCZ) and Palau's location near the Pacific Warm Pool, which leads to relatively high rainfall through the year.
- Annual and seasonal air temperatures at Koror increased over the period 1952–2017. The annual number of hot days and warm nights has increased, while the number of cool days and cold nights has decreased. The energy required for cooling indoor environments has also increased.
- There has been little change in annual, seasonal and extreme rainfall at Koror.
- Tropical cyclones can affect Palau year-round. Over the period 1969–2017, an average of 31 cyclones passed within Palau's exclusive economic zone (EEZ) per decade. Tropical cyclones were most frequent in neutral El Niño–Southern Oscillation (ENSO) years and least frequent in El Niño years. Year-to-year variability is large, ranging from no tropical cyclones in some years to nine in 1971.
- There has been little change in the number of severe tropical cyclones or the total number of tropical cyclones in the Northwest Pacific since 1981.

9.1.2 Ocean

- Highest sea levels typically occur in the months June–September.
- Sea-level rise at the EEZ, measured by satellite altimeters from 1993 to mid-2020, ranges from about 2 to 3.5 mm (0.08 to 0.14 in) per year.
- Monthly average sea surface temperature (SST) near Koror, as measured by satellite, ranges from approximately 28 °C (82.4 °F) in February to 29.4 °C (84.9 °F) in June. Monthly temperatures in any given year can be up to ±1.5 °C (± 2.7 °C) of these averages.
- The SST trend in the EEZ is 0.24 °C (0.43 °F) per decade.
- Dominant wave direction is from 80° (south), with an average significant wave height of 0.71 m (2.33 ft) and average wave period of 9.19 s.
- Severe wave height was defined as 1.61 m (5.28 ft), with an average of 3.7 severe events per year.
- Peak average significant wave height occurs between November and March.

9.2 Country description

The Republic of Palau is an archipelago located in the equatorial/tropical North Pacific Ocean (Figure 9.1). The nation has approximately 340 islands located between latitudes 3°N and 8°N, and longitudes 131°E and 135°E. Palau has a total land area of 466 km^2 and an EEZ of 0.6 million km^2. Babeldaob, the largest island at 331 km^2, includes the capital, Ngerulmud. The highest elevation is 242 m (794 ft) above sea level on Babeldaob. Palau's population is approximately 18,000. About two thirds of the population live on Koror.

Figure 9.1:
Palau and the location of the climate station used in this report

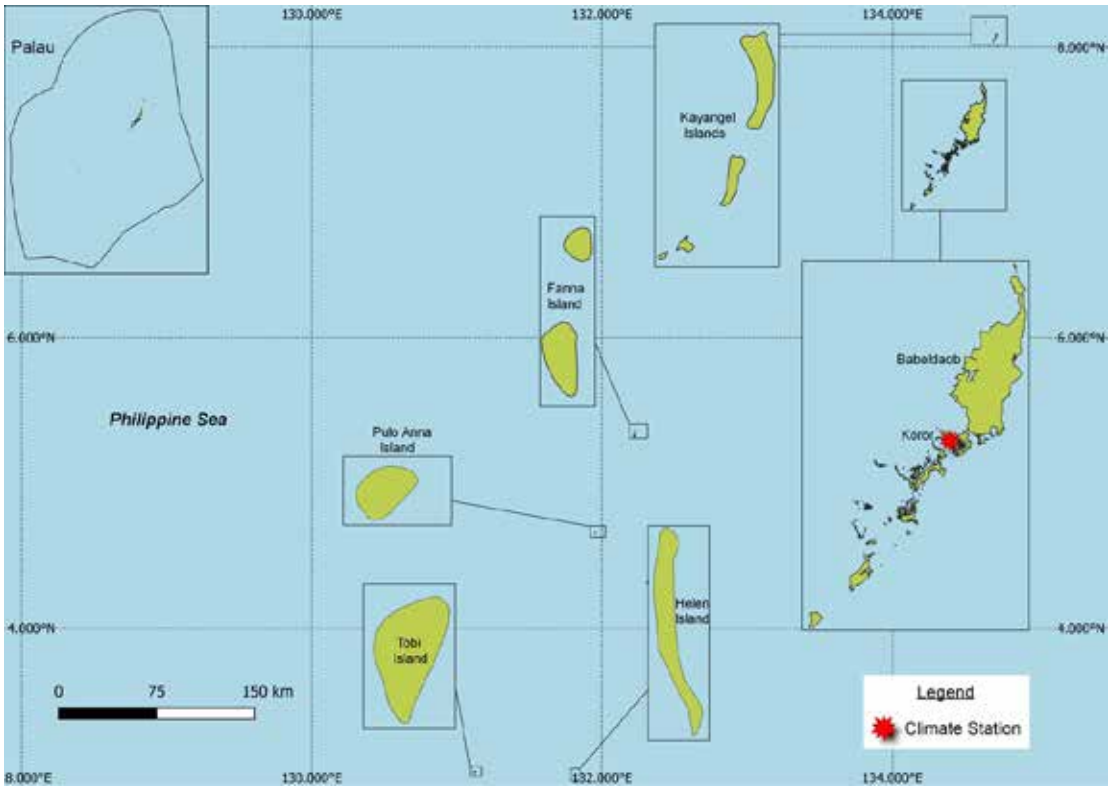

9.3 Data

Daily historical rainfall and air temperature records for Koror Weather Service Office from 1951 were obtained from the United States National Oceanic and Atmospheric Administration Palau Weather Service Office. These records have undergone data quality and homogeneity assessment. Where the maximum or minimum air temperature records were found to have discontinuities, these records have been adjusted to make them homogeneous (further information is provided in Chapter 1). Additional information on historical climate trends for Palau can be found in the Pacific Climate Change Data Portal http://www.bom.gov.au/climate/pccsp.

Tropical cyclone data and historical tracks starting from the 1969 season are available from the Western Northern Hemisphere Tropical Cyclone Data Portal http://www.bom.gov.au/cyclone/history/tracks/beta/?region=wnp.

SST covering the EEZ for Palau was obtained via the daily Optimum Interpolation SST version 2.1 (OISST v2.1) dataset from NOAA (Reynolds et al. 2007; Banzon et al. 2016).

Wave data were obtained from the PACCSAP wave hindcast (Smith et al. 2021), available hourly from 1979 to 2021, with a grid resolution near Palau of 7 km (4.3 mi).

Regional sea level data were obtained from CSIRO satellite altimetry (updated by Benoit Legresy, Church and White 2011), with correction for seasonal signals, inverse barometer effect and glacial isostatic adjustment. Tide-gauge data were sourced from the University of Hawaii Sea Level Center data archive for the Malakal tide-gauge station, spanning from 1990 to 2018 at hourly intervals.

9.4 Rainfall

9.4.1 Seasonal cycle

Palau's location on the edge of the Pacific Warm Pool and the year-long influence of the ITCZ lead to a relatively high average monthly rainfall. Koror's wet season is from May to October, which averages over 2100 mm (82.7 in) of rainfall or 58% or Koror's annual rainfall (Figure 9.2). The WPM is usually most active and brings heavy rainfall during these wet season months. March, the driest month, still averages 207 mm (8.1 in) of rainfall.

Winds are generally moderate, and the northeasterly trades prevail from December through to March. During April, the frequency of trade winds decreases, and there is an increase in the frequency of easterly winds. In May, the winds are predominantly from southeast to northeast.

Figure 9.2:
Mean annual rainfall at Koror

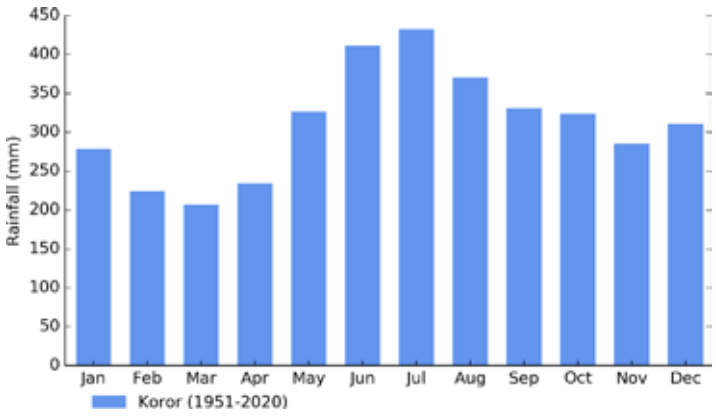

9.4.2 Trends

Trends in annual and seasonal rainfall since 1952 are not statistically significant at Koror (Figure 9.3, Table 9.1). Annual and seasonal rainfall trends indicate little change. Annual rainfall has varied from approximately 2500 to 5500 mm (98.4 to 216.5 in).

Figure 9.3:
Annual rainfall (bar graph) and number of wet days (where rainfall is at least 1 mm; line graph) at Koror. Straight lines indicate linear trends for annual rainfall (in black) and number of wet days (in blue). The magnitudes of the trends are presented in Table 9.1. Diamonds indicate years with insufficient data for one or both variables.

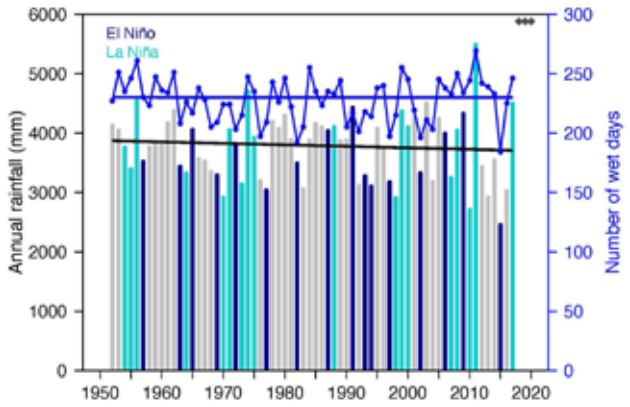

Table 9.1:
Trends in annual, seasonal and extreme rainfall at Koror. The 95% confidence intervals are shown in parentheses. The contribution to total rainfall from extreme events and the standardised rainfall evapotranspiration index are measured relative to 1961–1990 (see Chapter 1 for details).

	Koror
	1952–2017
Annual rainfall (mm/decade)	-24.92 (-103.73, +52.52)
November–April (mm/decade)	-1.43 (-51.70, +54.03)
May–October (mm/decade)	-33.22 (-83.83, +15.96)
Number of wet days (days/decade)	-0.01 (-3.52, +3.34)
Contribution to total rainfall from extreme events (%/decade)	-0.56 (-1.76, +0.63)
Consecutive dry days (days/decade)	0.00 (-0.21, +0.62)
Maximum one-day rainfall (mm/decade)	-4.73 (-10.67, +1.84)
Standardised rainfall evapotranspiration index (November–April)	0.00 (-0.17, +0.16)
Standardised rainfall evapotranspiration index (May–October)	-0.11 (-0.27, +0.07)

Similar to annual and seasonal rainfall, no significant trends in extreme rainfall indices, including the standardised rainfall evapotranspiration drought index, were detected (Table 9.1). Figure 9.4 shows change and variability in the longest run of days without rain and maximum daily rainfall at Koror. Some decade-to-decade variability in maximum daily rainfall is evident, and dry days rarely persist for longer than two weeks, consistent with Koror's tropical location.

Figure 9.4:
Annual longest run of consecutive dry days (bar graph) and maximum daily rainfall (line graph) at Koror. Straight lines indicate linear trends for dry days (in black) and maximum daily rainfall (in blue). The magnitudes of the trends are presented in Table 9.1. Diamonds indicate years with insufficient data for one or both variables.

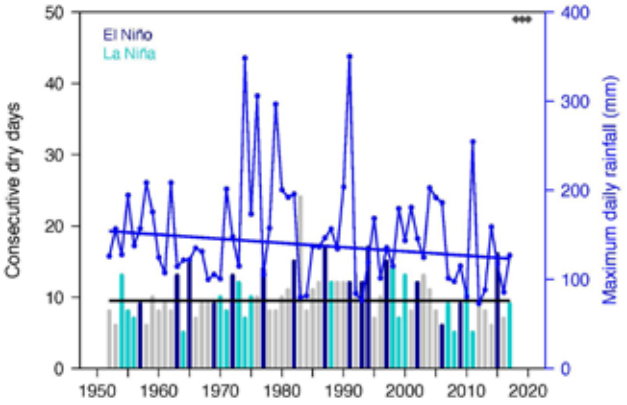

9.5 Air temperature

9.5.1 Seasonal cycle

Air temperatures in Koror have very little seasonal variation throughout the year and are strongly linked to changes in the surrounding ocean temperature. The maximum average temperature for Koror is around 32 °C (89.6 °F), with a minimum average temperature of approximately 25 °C (77.0 °F) and an average difference between the warmest and coolest months of less than 1 °C for both maximum and minimum temperatures (Figure 9.5). There has been a shift towards warmer average monthly temperatures for both maximum and minimum temperatures between the climatology periods of 1961–1990 and 1991–2020. Warmer average temperatures occurred in all months at Koror for the most recent climatology period. The largest increase in average maximum monthly temperatures occurred during the warmer/drier season (November–April).

Figure 9.5:
Maximum and minimum air temperature seasonal cycle for Koror (purple), and for the periods 1961–1990 (dotted lines) and 1991–2020 (solid lines).

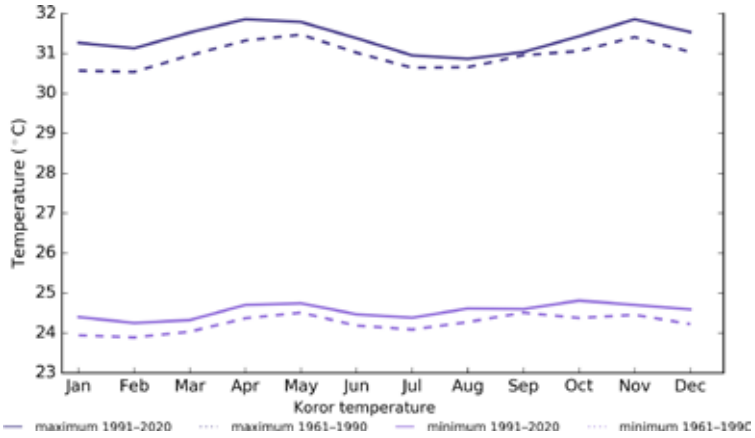

9.5.2 Trends

Average annual and seasonal temperatures have increased significantly at Koror (Figure 9.6, Table 9.2). November–April temperatures have increased faster than May–October temperatures. Year-to-year fluctuations in temperature are typically small and can be attributed to Koror's tropical location.

Figure 9.6:
Average annual, November–April and May–October temperatures for Koror. Straight lines indicate linear trends. The magnitudes of the trends are presented in Table 9.2. Diamonds indicate years with insufficient data for one or more variables.

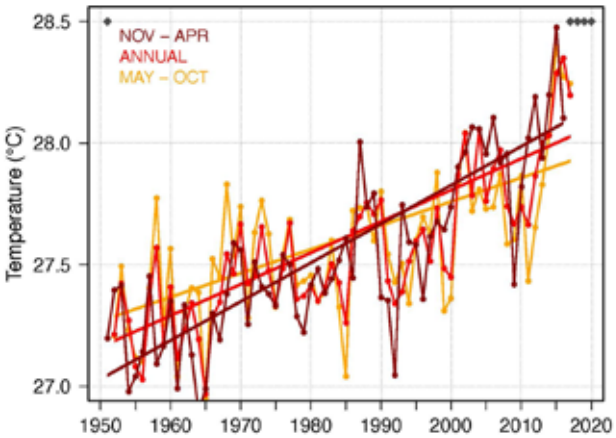

Table 9.2:
Trends in annual and seasonal air temperatures at Koror. The 95% confidence intervals are shown in parentheses, and trends significant at the 95% level are shown in bold.

	Koror Tmax (°C/decade)	Koror Tmin (°C/decade)	Koror Tmean (°C/decade)
	1952–2017		
Annual	**+0.13** (+0.09, +0.18)	**+0.10** (+0.03, +0.17)	**+0.13** (+0.08, +0.17)
November–April	**+0.18** (+0.13, +0.23)	**+0.13** (+0.07, +0.18)	**+0.16** (+0.12, +0.20)
May–October	**+0.08** (+0.04, +0.12)	**+0.10** (+0.03, +0.17)	**+0.10** (+0.05, +0.14)

The number of hot days and warm nights has increased, and the number of cool days and cold nights has decreased at Koror (Table 9.3, Figure 9.7). The number of hot days exhibits large decadal variability. This may be partly due to Koror's tropical location, which requires only small temperature changes for a day to be considered hot, i.e., in the top 10% of days compared to 1961–1990 (see Chapter 1 for details).

The cooling degree days index provides a measure of the energy demand needed to cool a building down to 25 °C (77.0 °F), with the assumption that air conditioners are generally turned on at this temperature. There has been a strong increase in the cooling degree index, suggesting the energy needed for cooling has increased significantly since 1952.

Table 9.3:
Trends in annual temperature extremes at Koror. The 95% confidence intervals are shown in parentheses, and trends significant at the 95% level are shown in bold. Hot and cool days, and warm and cold nights are measured relative to 1961–1990 (see Chapter 1 for details).

	Koror
	1952–2017
Number of hot days (days/decade)	**+13.69** (+7.99, +20.84)
Number of warm nights (nights/decade)	**+9.19** (+3.73, +14.51)
Number of cool days (days/decade)	**-4.30** (-5.92, 2.92)
Number of cold nights (nights/decade)	**-2.75** (-4.79, 0.69)
Cooling degree days (degree days/decade)	**+46.45** (+30.41, +61.43)
Daily temperature range (°C/decade)	+0.03 (-0.05, +0.13)

Figure 9.7:
Annual number of hot days and cold nights at Koror. Straight lines indicate linear trends. The magnitudes of the trends are presented in Table 9.3. Diamonds indicate years with insufficient data for one or both variables.

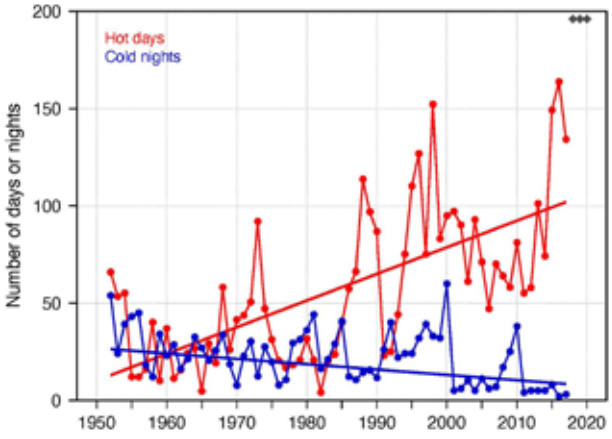

9.6 Tropical cyclones

9.6.1 Seasonal cycle

Tropical cyclones usually affect Palau year-round. The tropical cyclone archive of the western North Pacific indicates that between the 1969 and 2017 seasons, 153 tropical cyclones (Figure 9.8) passed within the EEZ. This represents an average of 31 cyclones per decade. Tropical cyclones were most frequent in neutral years (33 cyclones per decade), followed by La Niña years (31 cyclones per decade) and least frequent in El Niño years (29 cyclones per decade).

Interannual variability in the number of tropical cyclones in the EEZ is large, ranging from zero in some seasons to nine in 1971 (Figure 9.8). High interannual variability and the small number of tropical cyclones occurring in the EEZ make reliable identification of long-term trends in frequency and intensity difficult.

Some tropical cyclone tracks analysed in this section include the tropical depression stage (sustained winds ≤34 knots) before and/or after tropical cyclone formation.

Figure 9.8:
Number of tropical cyclones passing within the Palau EEZ per season. Each season is defined by the ENSO status, with light blue being an El Niño year, dark blue a La Niña year and grey showing a neutral ENSO year. The 11-year moving average is presented as a purple line and considers all years.

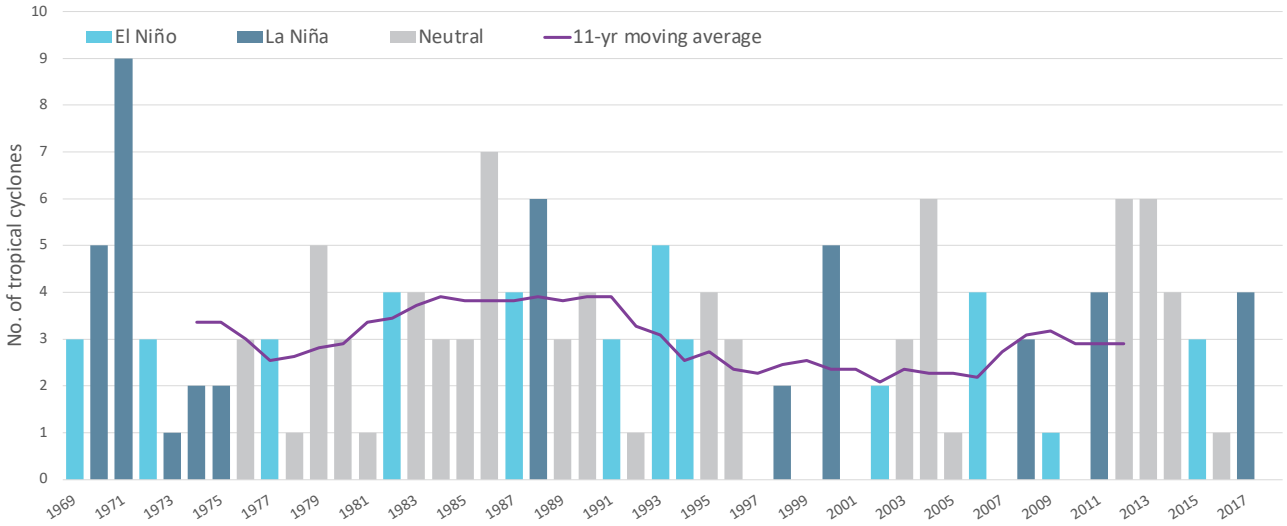

9.6.2 Trends

Trends in total number of tropical cyclones (<995 hPa) and severe tropical cyclones (<970 hPa) are presented for the period 1981–2021 for the Northwest Pacific (125°E–180°W; 0–20°N). Trends are presented at a regional scale as the number of tropical cyclones occurring within Pacific Island EEZs is insufficient for reliable long-term trend analysis.

For the total number of tropical cyclones, the trend (and 95% confidence interval) is -0.56 (-1.84, 0.72) tropical cyclones/decade. There has been little change in the total number of tropical cyclones over the last 41 seasons.

For the total number of severe tropical cyclones, the trend is -0.15 (-1.19, 0.89) tropical cyclones/decade. There has been little change in the number of severe tropical cyclones over the last 41 seasons.

There has also been little change in the proportion of tropical cyclones reaching severe status. The trend is 0.01 (-0.04, 0.05) tropical cyclones/decade.

Records of tropical cyclones exist from the late 1800s in some countries in the Northwest Pacific, but trends in tropical cyclones have only been presented from 1981/82. Satellite-based observations began in the early 1970s, but consistent coverage and reliable intensity estimates have only been available since the early 1980s. Confidence in tropical cyclone trends is moderate as the definition of a tropical cyclone has changed and satellite observation methods have continued to improve over the last 41 years.

9.7 Sea surface temperature

9.7.1 Seasonal cycle

Sea surface temperature, as measured by satellite observations near Koror from 1982 to 2021, reaches on average a maximum of 29.4°C (84.9 °F) in June and then reaches a secondary peak of 29.3 °C (84.7 °F) in November but can get as high as 30.6 °C (87.1 °F) in September (Figure 9.9). Minimum average temperature reaches almost 28 °C (82.4 °F) in February. Temperatures can be up to 1.5 °C (2.7 °F) higher or lower than these averages, although 50% of observations fall within 1.0 °C (1.8 °F) of the average.

Figure 9.9:
Annual temperatures near Koror from satellite observations. Blue dots show the monthly average, and shaded boxes show the middle 50% of observations. Lines show the top and bottom 25% of observations.

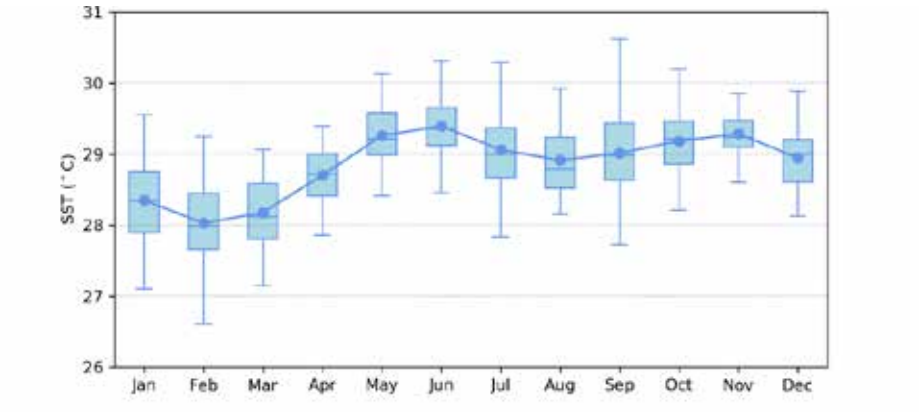

9.7.2 Trends

Figure 9.10 shows the 1981–2021 SST from satellite observations averaged over the Palau EEZ. The data show a trend of 0.24 °C (0.43 °F) per decade with a 95% confidence interval of ±0.05 °C (±0.09 °F).

Figure 9.10:
Sea surface temperature from satellite observations averaged across the Palau EEZ, shown as the orange line. The blue line shows the linear regression trend.

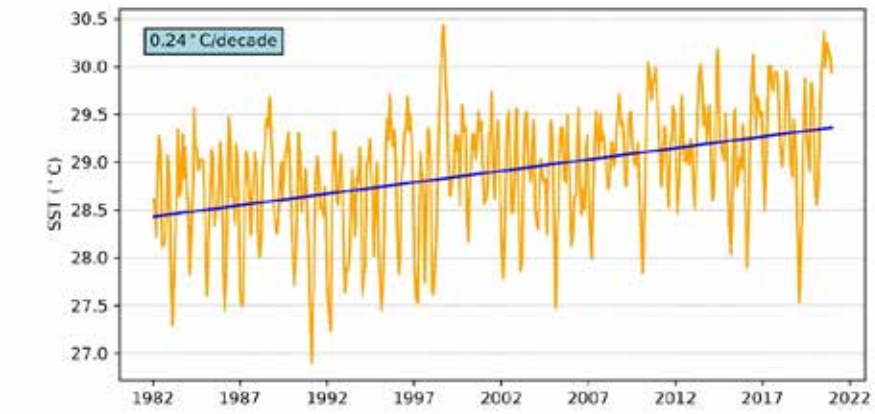

9.8 Sea level

9.8.1 Seasonal cycle

Palau experiences a semidiurnal tidal cycle, meaning two high and two low tides per day. The highest predicted tides of the year typically occur between July and October. Figure 9.11 shows the number of hours the 99th percentile (1.82 m, 5.97 ft) sea level threshold is exceeded per month across the entire sea level record at Malakal Island, Koror. Peak sea levels typically occur between June and September.

Figure 9.11:
Number of hours exceeding 99th percentile sea level threshold per month from 1990 to 2017 at the Malakal Island tide-gauge. Blue shading indicates the number of hours, and the final row provides a percentage summary of all the years.

Number of hours exceeding 1.82 m (Koror, Palau)

	Jan	Feb	Mar	Apr	May	Jun	Jul	Aug	Sep	Oct	Nov	Dec	Annual
1990	0	0	0	0	0	0	0	0	0	0	0	0	0
1991	0	0	0	0	0	0	0	0	0	0	0	0	0
1992	0	0	0	0	0	0	0	0	0	0	0	0	0
1993	0	0	0	0	0	0	0	0	0	0	0	0	0
1994	0	0	0	0	0	0	0	0	0	0	0	0	0
1995	0	0	0	0	0	0	0	0	0	0	0	0	0
1996	0	0	0	0	0	0	0	0	0	0	0	0	0
1997	0	0	0	0	0	0	0	0	0	0	0	0	0
1998	0	0	0	1	1	0	2	1	4	0	1	0	10
1999	0	0	0	0	0	0	8	0	0	0	0	1	9
2000	0	0	0	0	0	0	0	11	0	0	0	0	11
2001	2	2	1	2	1	0	0	0	0	0	0	0	8
2002	0	0	0	0	0	0	0	0	0	0	0	0	0
2003	0	0	0	0	0	0	0	0	0	0	0	0	0
2004	0	0	0	0	0	0	0	0	0	0	0	0	0
2005	0	0	0	0	0	0	0	0	0	0	0	0	0
2006	0	0	0	0	0	0	0	0	0	0	0	0	0
2007	0	0	0	0	0	0	0	0	0	0	0	0	0
2008	0	3	0	0	0	0	1	1	0	1	1	1	8
2009	0	0	0	0	0	0	0	0	0	0	0	0	0
2010	0	0	0	0	0	0	3	0	0	0	0	0	3
2011	0	0	5	0	0	0	0	0	1	0	0	0	6
2012	0	0	0	0	0	0	2	0	0	0	0	0	2
2013	0	0	0	0	0	16	15	0	9	2	2	2	46
2014	0	0	0	0	0	0	0	0	0	0	0	0	0
2015	0	0	0	0	0	0	0	0	0	0	0	0	0
2016	0	0	0	0	0	0	0	0	0	3	0	0	3
2017	0	0	0	0	0	0	0	0	0	0	0	0	0
Monthly Totals (%)	2	5	6	3	2	15	29	12	13	6	4	4	

9.8.2 Trends

Sea level at Palau, measured by satellite altimeters (Figure 9.12) since 1993, has risen between 2 and 3.5 mm (0.08 and 0.14 in) per year, with a 95% confidence interval between ±1 mm (±0.04 in) and ±1.8 mm (±0.07 in). Palau falls in the region with the highest uncertainty in trend estimates in the southern and western/central Pacific.

Figure 9.12:
The satellite altimetry annual trend for the Pacific from 1993 to 2020, with the Palau EEZ highlighted. The star symbol indicates the location of the tide-gauge at Koror.

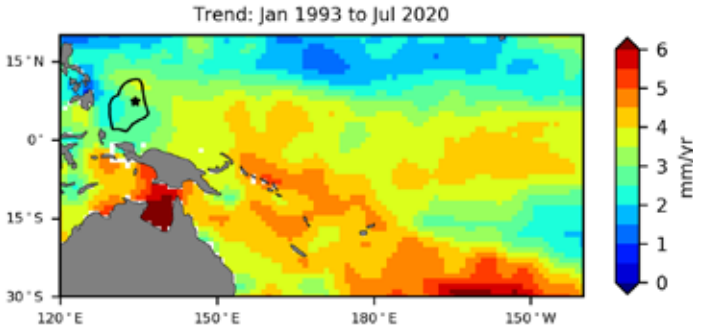

The Malakal Island tide-gauge has sea level data spanning from May 1969 to December 2018. A trend analysis of the data shows a rising trend of 2.31 mm (0.09 in) per year with a confidence interval of ±1.33 mm (±0.05 in), which is very similar to the altimeter trend shown at the location of the star symbol in Figure 9.12. An additional trend analysis was undertaken on the tide-gauge data to match as best as possible the time span of the altimetry, from January 1993 to December 2018. Over this shorter period, the trend becomes 4.89 mm (0.19 in) per year with a confidence interval of ±1.9 mm (±0.07 in), which is higher than the altimetry estimates, suggesting that subsidence has been occurring at Palau in recent decades.

9.9 Waves

9.9.1 Seasonal cycle

The average wave climate in Koror is defined by the significant wave height, peak period and peak direction. The significant wave height is the mean wave height (from trough to crest) of the highest one third of waves and corresponds to the wave height that would be reported by an experienced observer. Peak period is the time interval between two waves of the dominant wave period. Peak direction is the direction from which the dominant waves are coming.

The average sea state is dominated by wind seas from the east. The annual mean wave height is 0.71 m (2.32 ft), the annual mean wave direction is 80° and the annual mean wave period is 9.19 s. In the Pacific, waves often come from multiple directions and for different periods at a time. In Koror, there are often more than three different wave direction/period components coming from the southeast to southwest (Figure 9.13).

Figure 9.13:
Annual wave rose for Koror. Note that direction is where the wave is coming from.

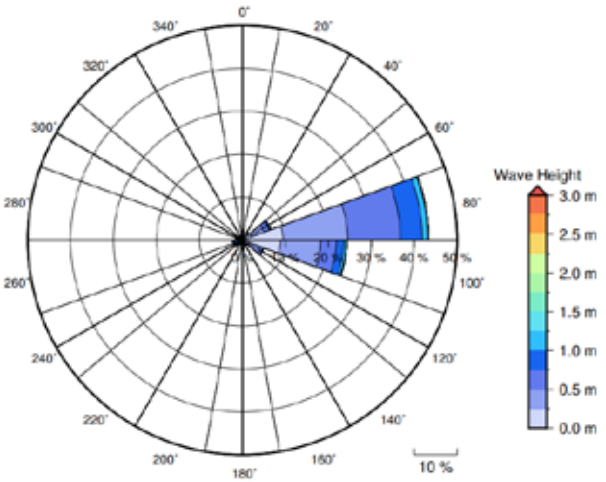

Seasonal wave activity peaks between December and March in terms of both wave height and period (Figure 9.14) due to North Pacific extra-tropical storm activity. Conversely, there is a distinct lull between May and October in wave activity.

Figure 9.14:
Monthly wave height (black line), wave period (red line) and wave direction (arrows). The grey area represents the range of wave height between calm periods (10% of lowest wave height) and large wave events (10% of highest wave height).

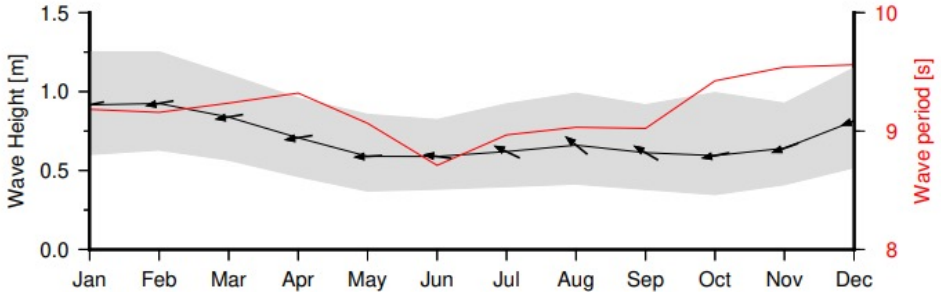

9.9.2 Trends

Waves change from month to month with the seasons, but they also change from year to year with climate oscillations. Typically, these changes are smaller than the seasonal changes but can be important during phenomena such as ENSO. In Koror, the mean annual wave height has remained unchanged since 1979 (Figure 9.15). The mean annual wave height in Koror is not significantly correlated with the main climate indicators of the region.

Figure 9.15:
Annual wave height (black line), wave period (red line) and wave direction (arrows). The grey area represents the range of wave height between calm periods (10% of lowest wave height) and large wave events (10% of highest wave height).

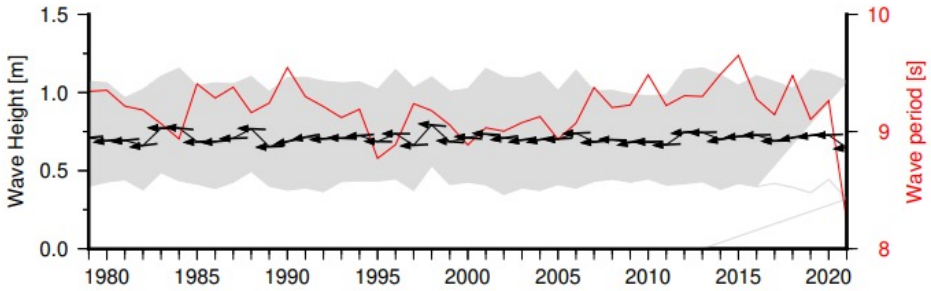

9.9.3 Extreme waves

Extreme wave analysis completed for Koror was done by defining a severe height threshold and fitting a generalized Pareto distribution (GPD). The optimum threshold selected was 1.61 m (5.28 ft). In the 42-year wave hindcast, 155 wave events reached or exceeded this threshold, averaging 3.7 per year. The GPD was fitted to the largest wave height reached during each of these events (Figure 9.16, Table 9.4). Extreme wave analysis is a very useful tool but is not always accurate because the analysis is very sensitive to the data available, the type of distribution fitted and the threshold used. For example, this analysis does not accurately account for tropical cyclone waves. More in-depth analysis is required to obtain results appropriate for designing coastal infrastructure and coastal hazard planning.

Figure 9.16:
Extreme wave distribution for Koror. The crosses represent the wave events that have occurred since 1979. The solid line is the statistical distribution that best fits past wave events. The dashed lines show the upper and lower confidence limits of the fit. There is a 95% chance that the fitted distribution lies between the two dashed lines. Note that the annual return interval is in logarithmic scale.

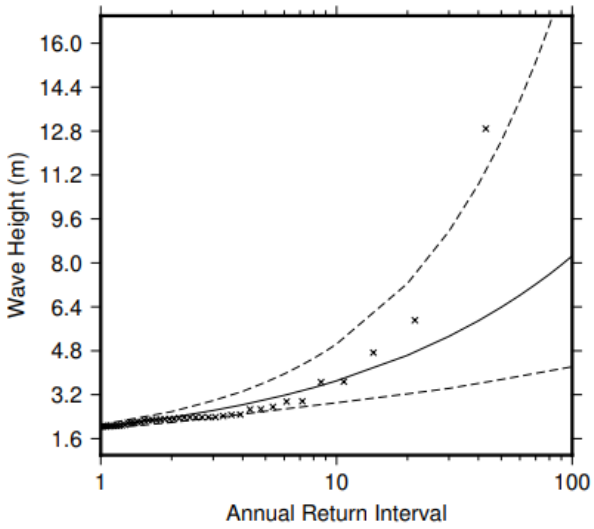

Table 9.4:
Summary of the results from extreme wave analysis in Koror

Large wave height (90th percentile)	1.07 m (3.51 ft)
Severe wave height (99th percentile)	1.54 m (5.05 ft)
1-year ARI wave height	2.03 m (6.66 ft)
10-year ARI wave height	3.70 m (12.14 ft)
20-year ARI wave height	4.64 m (15.22 ft)
50-year ARI wave height	6.38 m (20.93 ft)
100-year ARI wave height	8.25 m (27.07 ft)